

UDC 621.384.6:620.198

DOI: 10.15587/1729-4061.2016.65424

*Досліджено процес гомогенізації порошку діоксиду цирконію в конвективному осередку при вакуумно-дуговому виготовленні реакторних сталей. Процес запропоновано здійснювати застосуванням катоду з поперечним перерізом типу «fish-bone». Аналізується вплив форми катоду, розміру легуючих частинок, масопереносу в конвективному осередку з неплоским профілем дна і вільними межами на рівномірність розподілу діоксиду цирконію в розплаві сталі*

*Ключові слова: реакторна сталь, порошок оксиду, катод, вакуумно-дуговий переплав, гомогенізація, конвективний масоперенос*

*Исследован процесс гомогенизации порошка диоксида циркония в конвективной ячейке при вакуумно-дуговым изготовлении реакторных сталей. Процесс предложено осуществлять применением катода с поперечным сечением типа «fish-bone». Анализируется влияние формы катода, размера легирующих частиц, массопереноса в конвективной ячейке с неплоским профилем дна и свободными границами на равномерное распределение диоксида циркония в расплаве стали*

*Ключевые слова: реакторная сталь, порошок оксида, катод, вакуумно-дуговой переплав, гомогенизация, конвективный массоперенос*

# INVESTIGATION OF THE OXIDE PHASE HOMOGENIZATION IN THE CONVECTIVE CELL WHILE PRODUCING VACUUM-ARC REMELTING

**L. Bozbiei**

Postgraduate student

A. N. Podgorny Institute of Mechanical Engineering Problems of NAS of Ukraine  
Dm. Pozharsky str., 2/10, Kharkiv, Ukraine, 61046  
Junior researcher\*

E-mail: bozbiei@kipt.kharkov.ua

**B. Borts**

Doctor of Technical Science, Senior Researcher  
Deputy Director  
Scientific Work\*

«Accelerating nuclear systems»\*\*

E-mail: borts@kipt.kharkov.ua

**I. Neklyudov**

Doctor of Physics & Mathematics Sciences,  
Professor, Academician of the NAN of Ukraine  
General director\*\*

E-mail: neklyudov@kipt.kharkov.ua

**V. Tkachenko**

Director\*

Doctor of Physics & Mathematics Sciences,  
Professor, Head of the Department  
Department of Physics of Innovative Energy &  
Technology & Ecology

V. N. Karazin Kharkiv National University  
Svobody sq., 6, Kharkiv, Ukraine, 61022

E-mail: tkachenko@kipt.kharkov.ua

\*Sci. & Production Establishment

«Renewable Energy Sources & Sustainable Technologies»\*\*

\*\*National Science Center

«Kharkiv Institute of Physics and Technology» of NAS of Ukraine  
Akademicheskaya str., 1, Kharkiv, Ukraine, 61108

## 1. Introduction

Powder metallurgy (PM) is the area of theoretical and practical knowledge, which describes methods of the key components manufacturing such as metal powders, alloys and metallic compounds, semi-finished products and their products as well as non-metallic powder production without melting the main component [1, 2].

PM includes the following main groups of operations: production of the starting metal powders and batch prepara-

tion; compacting powders (or mixtures thereof) in the preforms; sintering the resulting pieces.

The materials formed by the PM methods are called powder materials. These materials can be divided into the following types associated with their performance: structural, tribological, filtering, hard alloys, high temperature, electrical etc.

PM with specific nuclear properties (B, Hf, Cd, Zr, W, Pb, REE and other their compounds) are used in nuclear power as scavengers and inhibitors. Control rods, fuel rods

of the dioxide-based powders, carbides, uranium nitrides and powders of refractory compounds of other transuranic elements [3] are made of them.

---

## 2. Analysis of published data and problem statement

---

Recently, the PM is used for production of the oxide dispersion strengthened (ODS) steels which are utilized as materials of construction, radiation-resistant and heat-resistant components of nuclear facilities [4].

PM is the traditional method for production of ODS steels [5]. ODS steels contain particles of nanometer size oxide with high density, enriched with yttrium, oxygen, manganese, chrome and silicon.

The effect of neutron irradiation and temperature on particles behavior was investigated for different kinds of ODS steels, for example, Eurofer [6] and Eurofer 97 Ferritic-Martensitic [7]. These particles play the key role in the increase of strength of the material and improvement of radiation resistance – pinning of dislocation.

Investigations in this direction given encouraging results.

However, technology of obtaining of ODS steel by methods of PM is characterized by such disadvantages as a large number of procedures of raw-materials preparation, high demands to their purity and granulometry. Rather high cost of metallic powders and impossibility of producing the ingots of large sizes can also be added to these disadvantages.

The method of vacuum-arc remelt on the example of *08X18H10T* steel with addition of  $ZrO_2$  [8] is the alternative technology of obtaining the ODS steels which is under development in the last time.

When realizing this technology, according to visual observations, forming of the convective cell from the melted metal is necessary to consider.

Therefore, in this paper, it is offered to consider the process of vacuum-arc remelt of the *08X18H10T+ZrO<sub>2</sub>* steel, based on the process taking part in the incompressible, heated from below (above) viscous liquid on condition that elementary convective cell (ECC) [9] is formed in the melted metal. Based on the obtained in the paper [8] spatial distribution of the liquid rate in the ECC, criteria of homogenization of zirconium oxide particles over the volume of the ODS steel sample were offered.

However, achievement of the needed level of homogeneity of  $ZrO_2$  powder distribution in the metal volume, described in [8], is complicated with a number of reasons.

One of them lays in the fact that the unevenness of  $ZrO_2$  powder intake into the melt results from filling of the whole cylindrical volume of the aperture with zirconium dioxide powder. Such filling (while filling the axis of the aperture is placed vertically) results in the fact that in operating condition the axis of the aperture takes the horizontal position. In the result of melting of the steel plug isolating the aperture, volley discharge of the powder till the moment the angle of natural slope is formed which depends on the size of the particles and density of zirconium oxide powder.

The second reason of unevenness of zirconium dioxide intake into the melt is connected with the fact that the azi-

imuth angle of the cylindrical apertures axis in relation to the cathode axis cannot always be the same, as while production definite tolerances and inaccuracies exist.

Thus, the paper presents discussions of demands to the placement of  $ZrO_2$  powder in the cathode, which should be taken into consideration while producing the ODS steel by the method of vacuum-arc remelt in order to provide the high level of homogenization of the oxide particles.

---

## 3. Purpose and objectives of the study

---

The purpose of this paper is an analytical study of homogenization processes of the oxide phase by mass transfer in the convective cell, which is formed in the mold during the reactor steels vacuum-arc manufacturing.

To achieve this goal, it is necessary to solve the following problems:

- provide the design of the vacuum-arc furnace cathode and describe conditions of uniform admission  $ZrO_2$  powder into the melt;
- calculate the spatial distribution of the convective mass transfer rate of the liquid metal in a cylindrical cell with a non-planar bottom profile and free boundary conditions;
- define the  $ZrO_2$  powder particle size, when the spatial homogenization thereof is observed;
- describe in general the scenario of the vacuum arc melting and convective homogenization of the  $ZrO_2$  nanoparticles under vacuum arc steel ODS production.

---

## 4. Description of the experimental facility for vacuum-arc remelting of steel alloyed with oxide nano-powders

---

Scheme of obtaining the ODS steels by means of arc re-melt in the volume of liquid metal with distributed in it nano- or micro-dispersed  $ZrO_2$  particles is presented in Fig. 1 [8]. According to this scheme, crystallizer works as the anode, produced from copper and constitutes cylindrical glass with diameter 0.06 m. Crystallizer is cooled with flowing water from the external side. Steel cylindrical cathode with diameter  $D = 2R_0 = 0.03$  m and height  $H = 0.20 \dots 0.25$  m is loaded into the crystallizer. Cylindrical apertures, fully filled with dispersion particles of  $ZrO_2$  with diameter 0.003–0.005 m are drilled in cathode transversely to its axis, evenly on the azimuth and its length. Apertures are sealed with the plugs from the same steel. Electric arc is burnt and kept between anode and cathode. Support of arc burning is conducted due to moving of the cathode upwards along the glass axis. Steel melt flowing down over the electrode surface captures  $ZrO_2$  particles and creates a drop which is kept on the electrode lower ledge by surface tension forces.

Excess of the critical mass of the drop results in its separation and falling on the surface of the remelt, creating the horizontal cylindrical layer of the melted metallic composite metal +  $ZrO_2$  particle in the form of a liquid bath. Melting is conducted in vacuum  $10^3$  Pa. Water-cooled bottom and internal wall of the copper crystallizer favors quick crystallization of the melt, which takes place within 20–30 minutes.

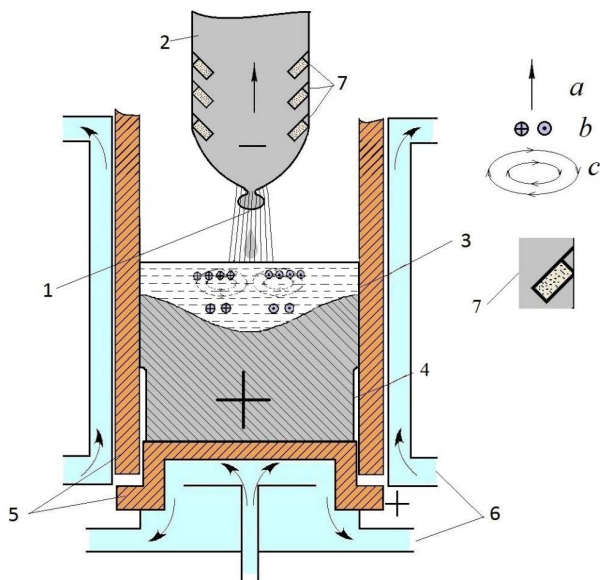


Fig. 1. Motion of liquid metal when fusing the ingot in vacuum-arc furnace: *a* – direction of the electric current; *b* – circular motion of the metal in the horizontal plane; *c* – motion of metal in the vertical plane; 1 – corona; 2 – electrode (cathode) which is melted; 3 – liquid metal; 4 – ingot; 5 – copper crystallizer (anode); 6 – cooler (water); 7 – cavities with alloying add-mixture

### 5. Description of the cathode construction

The present work, unlike the described earlier in [8] scheme of steel cathode with embedded zirconium dioxide particles for provision of better homogenization of zirconium oxide powder, presents a different scheme.

A new scheme of  $ZrO_2$  powder disposition in the cathode is presented in Fig. 1, 2. In accordance with this scheme, in-line circular grooves with width  $\Delta x$  appear on the surface of the steel cathode 1, whose bottom generative constitutes together with radius the angle equal to the friction angle of zirconium dioxide  $\varphi$  (Fig. 2). Such grooves can be created with the set of washers 2 of a special form from the same metal as the cathode which are densely pressed on the cathode. Prepared for vacuum melting cathode creates the structure of “fish-bone” type with height  $H = 0.20 \dots 0.25$  m in the axial section. Axis slope angle of circular grooves  $\alpha$  in relation to the cathode radius is determined experimentally. In our case, it was selected so that it was significantly less than the friction slope of zirconium dioxide powder  $\varphi$  and provided the absence of powder precipitation during vibration while melting. The scheme of “fish-bone” axial section is presented in Fig. 2. In order to prevent precipitation of zirconium oxide powder from the cathode grooves while shifting, connected with its installation in a vacuum chamber, the whole “fish-bone” system is pressed in the thin-walled cylindrical tube 3, produced from the steel of the same type.

The design of the cathode, proposed in Fig. 2 provides even entry of oxide powder in the melt volume within the whole period of vacuum-arc melting. In order to conduct full description of the cathode parameters packed density of zirconium dioxide, friction slope  $\varphi$  and also slope angle of circular grooves axis  $\alpha$  in relation to cathode radius which according to our calculations should be significantly less  $\varphi$ ,

that is  $\varphi \gg \alpha$  should be assigned. The last condition is needed for prevention of simultaneous entry of zirconium dioxide powder from two circular grooves, placed one over another.

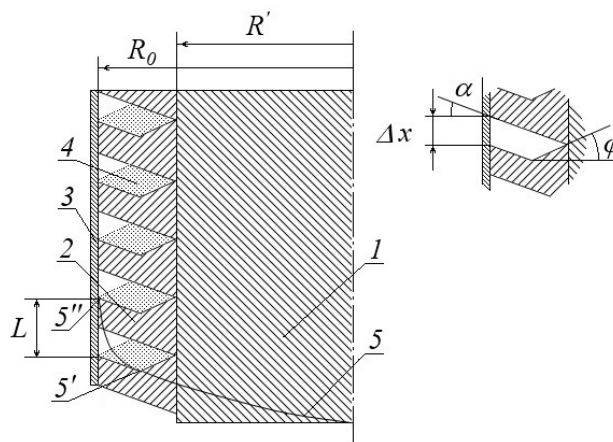


Fig. 2. Design of the cathode for vacuum-arc melting of ODS steel: 1 – cylindrical cathode with radius  $R'$ ; 2 – washer of special form with external radius  $R_0$ ; 3 – thin-walled cylindrical tube; 4 – micro or nano-dispersed particles of  $ZrO_2$ ; 5 – cathode melting line; 5' – point of completion of  $ZrO_2$  particles precipitation from the circular groove; 5'' – point of start of  $ZrO_2$  particles precipitation from the circular groove

In order to provide evenness of  $ZrO_2$  powder entry, we should know its physical parameters.

They will be described below.

### 6. Physical properties of zirconium dioxide powder

#### Packed density.

Research of the zirconium dioxide powders formation showed that calcination without preliminary drying promotes formation of more dense particles in comparison with preliminary dried. It is confirmed by the values of their packed density and tap density, which correspondingly constitute for the non-dried powders  $1.65\text{--}1.75$  g/cm<sup>3</sup> and  $1.9\text{--}2.0$  g/cm<sup>3</sup>. For the powders calcined after drying, these values constitute correspondingly  $1.15\text{--}1.2$  g/cm<sup>3</sup> and  $1.4\text{--}1.45$  g/cm<sup>3</sup> [10, 11].

Packed density  $\rho_{ZrO_2} = 2.76$  g/cm<sup>3</sup> is characteristic for zirconium dioxide obtained by the method of vacuum drying from zirconium hydroxide [12].

*A repose angle of zirconium dioxide powder.* The angle of repose is an angle created by the free surface of the loose mountain mass or other free-flowing material with the horizontal plane. Sometimes the term “angle of internal friction” can be used. Material particles, placed on the free surface of the mound, undergo the condition of critical (limit) equilibrium. The angle of friction is connected with the friction coefficient and depends on the roughness of grains, the level of their moistening, grain composition and form and also on the relative density of the material.

When determining the friction angle, the bulk material is freely poured on the horizontal surface in the form of cone-shaped mountain. The angle between the generative and the basis of this cone is called the friction slope. The higher the

flowability of the powder the less is the angle of the friction slope. The angle of repose for powder- like and granular polymer materials is placed, as a rule, in the interval from 30° to 50°. The angle of repose for the materials with good flowability is less than 40° [11].

Zirconium dioxide right after its obtaining by the method of vacuum drying [12] is characterized by the angle of repose about 38°.

*ZrO<sub>2</sub> powder particle size.* Particle size of zirconium dioxide obtained by the method of vacuum drying is varied in the range 0.07...10 μm [12]. There are no conglomerates in the obtained powder.

### 7. Role of convective processes in homogenizing of nano-particles when obtaining the ODS steel

The process of vacuum-arc melting of steel, alloyed with oxide nano-powders is similar to described in [8]. At this, as it is mentioned in this paper, homogenizing of oxide nano-particles is conducted as a result of heat mass transfer of the melted steel on the crystallizer volume. Here, the vertical and horizontal velocities of the liquid steel mass transfer were estimated by their values in the elementary convective cell with the horizontal bottom and free boundary conditions [9].

However, in real conditions, it should be taken into account that the bottom of the cell is not plain and has a deflected profile whose generating line can be approximately presented in the form of some function of the radius. Besides this, as it goes from [13], the form of boundary conditions on the lower cell interface depends considerably on the quantity of the added highly dispersed phase. When adding less than 0.125 mass. % of the highly dispersed phase, solid boundary conditions are realized at the bottom of the cell, and when adding more quantity (more than 1.5 mass. %) – free boundary conditions are realized.

Let's study below homogenizing of ZrO<sub>2</sub> of highly dispersed phase in the melted stainless steel by means of convective mass transfer in the convective cylindrical cell with non-plate profile of the bottom and free boundary conditions.

### 8. Demands to the parameters of the cathode for vacuum arc melting of ODS steel

For realization of free boundary conditions, nano-dispersed powder of zirconium dioxide in the quantity more than 1.5 mass. % should be added into liquid metal melt. This demand provides specific conditions to the scheme of the internal structure of the cathode presented in Fig. 2.

The mass of zirconium dioxide powder  $M_{ZrO_2}$ , concentrated in the inclined circular groove is determined by the expression:

$$M_{ZrO_2} = \pi R_0^2 \Delta x \rho_{ZrO_2} \left( 1 - \frac{R'^2}{R_0^2} - \frac{2R'\Delta x}{R_0^2 \text{tg}\phi} \right) \quad (1)$$

When obtaining the expression (1), mentioned earlier condition  $\phi \gg \alpha$  is taken into account, and also the condition of the small width of the inclined circular groove  $\Delta x/R_0 \ll 1$ .

We assume that cutting period of the inclined circular grooves on the cathode is equal to L and their quantity N

is big, so the ration  $LN=H$  where  $N \gg 1$  is realized. Further everywhere during the calculations for the purpose of distinctness, we assume  $N=10$ .

The mass of the steel ingot is estimated by the value  $M_{St} = \pi R_0^2 H \rho_{St}$ ,  $\rho_{St} = 7.27 \text{ g/cm}^3$  – density of the stainless steel.

Thus, in order to implement the free boundary conditions in the elementary convective cell, the following relation should be realized:

$$\frac{M_{ZrO_2}}{M_{St}} = \frac{N \Delta x \rho_{ZrO_2}}{H \rho_{St}} \left( 1 - \frac{R'^2}{R_0^2} - \frac{2R'\Delta x}{R_0^2 \text{tg}\phi} \right) = \gamma X \left( 1 - Z^2 - \frac{2X \cdot Z}{\text{tg}\phi} \right) \geq 1.5 \cdot 10^{-2}, \quad (2)$$

where  $X = \frac{\Delta x}{R_0}$ ,  $\gamma = \frac{NR_0 \rho_{ZrO_2}}{H \rho_{St}}$ ,  $Z = \frac{R'}{R_0}$ .

Even entry of zirconium dioxide powder in the melt volume is realized on condition that the points 5'' and 5' are located at the cathode melting line 5, presented in Fig. 2. In order to achieve this condition, we assume cathode melting line 5 specified in the form:  $\beta_{St} = \beta/R_0$  – constant for this metal value,  $\beta$  – dimensionless constant determined experimentally.

Based on the above-mentioned, condition of even entry of zirconium dioxide powder the melt volume has the following form:

$$\frac{H}{NL} = \frac{H/NR_0\beta}{\left( 1 - \frac{R'^2}{R_0^2} - \frac{2R'\Delta x}{R_0^2 \text{tg}\phi} \right)} = \frac{\delta/\beta}{\left( 1 - Z^2 - \frac{2ZX}{\text{tg}\phi} \right)} = 1, \quad (3)$$

where  $\delta = \frac{H}{NR_0}$ .

Mutual solution of the inequality (2) on the lower limit and equation (3) for the parameters values  $\beta=3.5$ ,  $\gamma=0.28$ ,  $\delta=1.33$  corresponding to the conditions of the experiment, provides the following values of dimensionless width of the inclined circular groove and the relation of the internal diameter of the washer to the radius of cylindrical cathode  $X=0.14$  and  $Z=0.63$  correspondingly.

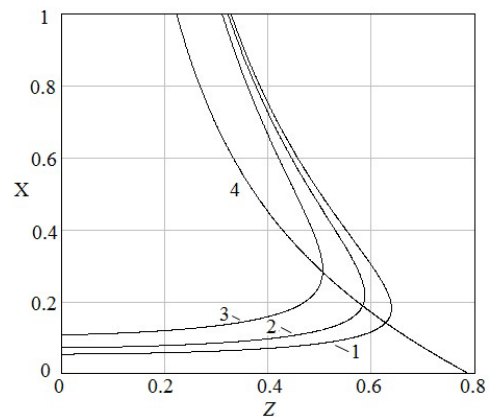


Fig. 3. Dependence of dimensionless width of the inclined circular groove X from the relation of internal radius of the washer to the radius of the cylindrical cathode Z. Curves: 1 – 1.5 mass. %; 2 – 2 mass. %; 3 – 3 mass %; 4 – condition of even entry of zirconium dioxide in the melt volume

Fig. 3 presents curves describing conditions of provision of free boundaries on the bottom of the cell when adding different quantities of powder  $ZrO_2$  (curves 1–1.5 mass. %; 2–2 mass. %; 3–3 mass %) and condition of even entry of zirconium dioxide in the melt volume (curve 4). Crossing points of curves 1–3 with 4 determine the value of dimensionless width in the inclined circular groove and relation of internal radius of the washer to the radius of the cylindrical cathode which provide free boundary conditions and evenness of  $ZrO_2$  powder entry into melted metal.

Thus, it is shown in the present section, that corresponding selection of cathode parameters, taking into account the physical properties of nano-dispersed powder  $ZrO_2$ , provides the uniform admission of the powder into the volume of melted metal.

### 9. Structure of the elementary convective cell with non-plane bottom profile

In order to describe the structure of the elementary convective cell (ECC) with non-plane bottom profile, we will study the cylindrical convective cell with a lower boundary placed in boundless along the axis  $x$  and  $y$  layer of viscous incompressible liquid with thickness  $h$  described with rotating surface with generating line:

$$z = -\left(\cos(\pi r R_c^{-1}) + 1\right) \Delta h / 2, \tag{4}$$

which has a common axis with the cylindrical cell. Here  $R_c$  is the radius of the cylindrical elementary convective cell,  $\Delta h$  is the largest deviation of the non-plane lower boundary of the cell. Axis  $z$  is directed upwards, perpendicular to the layer boundaries  $z=0$  and  $z=h$  (Fig. 4).

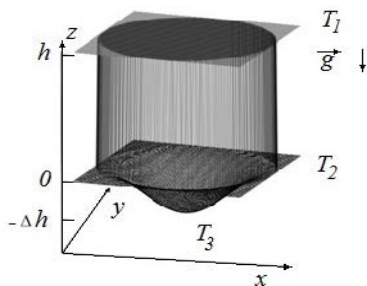


Fig. 4. Scheme of location of cylindrical elementary convective cell with radius  $R_c$  in the layer of viscous incompressible liquid with thickness  $h$  cosine bottom profile

Distribution of temperature over the layer thickness  $T_0(z)$  is assumed to be by a linear function from  $z$  coordinate. The temperature of the lower boundary of the cell is higher than the temperature of the upper boundary:  $T_0(0) = T_2$ ,  $T_0(h) = T_1$ , ( $T_2 > T_1$ ), and the temperature of the lower boundary point is equal to

$$T_0(-\Delta h) \equiv T_3 = T_2 + \Delta T_{bot} \quad (\Delta T_{bot} > 0).$$

Due to absence of disturbances, the linear dependence of the temperature on  $z$  coordinate provides the following values of its gradients:

$$\bar{\nabla} T_0(z) = -\frac{\Theta}{h} \bar{e}_z \quad (0 \leq z \leq h),$$

$$\bar{\nabla} T_0(z) = -\frac{\Delta T_{cone}}{\Delta h} \bar{e}_z \quad (-\Delta h \leq z \leq 0), \tag{5}$$

where  $\Theta = T_2 - T_1$  is the difference of temperatures between lower and upper planes,  $\bar{e}_z$  is the unit vector directed along the axis  $z$ ,  $\Delta T_{bot} = \Theta \Delta h / h$ .

### 10. Spatial distribution of convective mass transfer in ECC with non-plane bottom profile

Stokes line  $\psi_{1,2}(r, z)$  of the cylindrical cell with non-plane profile of the bottom and free boundary conditions, according to the Fujiwhara effect, similar to the task studied in [14] for ECC with the conic bottom profile, will be determined by superposition of Stokes functions of two vortices. One vortex describes in the cylindrical cell with plane free boundaries, second – in cylindrical cell with non-plane profile of the bottom and free boundaries:

$$\psi_{1,2}(r, z) = A_0 \left( 1 - \vartheta_{1,2} \left( z \frac{1 + \Delta h}{\Delta h}, r \right) \right) \psi_0(r, z, \Delta h), \tag{6}$$

where

$$\psi_0(r, z) = r \frac{R_c}{\sigma_{1,1}} \sin\left(\frac{\pi}{\Delta h} z\right) J_1\left(\frac{\sigma_{1,1}}{R_c} r\right),$$

where  $\sigma_{1,1}$  is the first zero of the Bessel function of the first order of the first type,

$$\vartheta_1(r, z) = J_0\left(\sigma_{0,1} \left( z / \Delta h - (\cos(\pi r / R_c) - 1) / 2 \right)\right)$$

and

$$\vartheta_2(r, z) = \cos\left(\left( z / \Delta h - (\cos(\pi r / R_c) - 1) / 2 \right) \pi / 2\right)$$

are the model functions providing free boundary conditions in the bottom of the cell with cosine profile.

Fig. 5 presents the Stokes lines for the free cylindrical elementary convective cell with cosine deep bottom with maximal depth  $\Delta h = 1/3$  in the result of the Fujiwhara effect usage (imposition of two vortices in the cell).

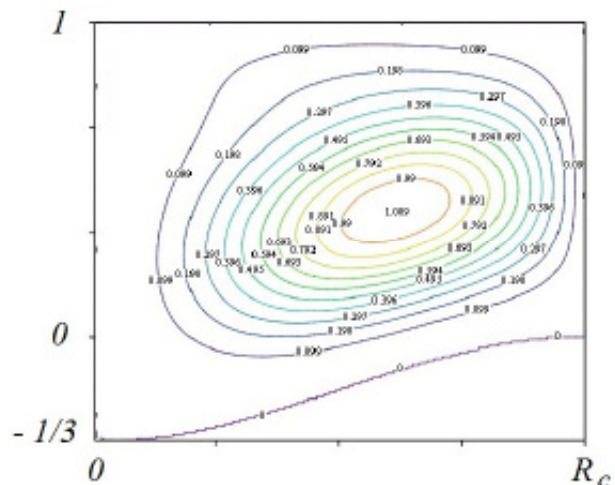


Fig. 5. Distribution of Stokes lines in the free cylindrical elementary convective cell with cosine deep bottom profile with maximal depth  $\Delta h = 1/3$  for model function  $\vartheta_1(r, z)$

Calculations show that for model functions  $\vartheta_1(r,z)$  and  $\vartheta_2(r,z)$ , the Stokes lines constitute concentrically placed smoothed, closed lines, whose form reflects deflected cosine bottom profile. Such view of the Stokes lines, in the same way as it is mentioned for the conic profile of the bottom [14], indicates the formation convective flux in the form of one vortex in the cell with free boundary conditions.

### 11. Sizes of ZrO<sub>2</sub> particles and conditions of their homogenization in the volume of ODS steel

Melting process of ODS steel melting can be studied on the example of convective motion of nano- or fine-dispersed inclusions from ZrO<sub>2</sub> in the volume of stainless steel 08X18H10T transferred into liquid condition.

Stainless steel stays in the liquid state under temperature under the temperature 1450÷1600 °C. Its density and kinematic viscosity are equal to  $\rho_1 = 7.27 \cdot 10^3$  kg/m<sup>3</sup> and  $\nu = 10^{-6}$  m<sup>2</sup>/s correspondingly [15]. Under such temperatures nano- or fine-dispersed inclusions from ZrO<sub>2</sub> in the liquid metal will be staying in solid phase as the melting temperature of ZrO<sub>2</sub> is determined by the value (0.75÷1)·2700 °C and significantly higher than the melting temperature of stainless steel [16, 17]. The density of ZrO<sub>2</sub> takes the value in the range  $\rho_p = (5.4 \dots 5.7) \cdot 10^3$  kg/m<sup>3</sup> and is always less than the density of liquid steel.

For analyses of homogenization of nano-particles of ZrO<sub>2</sub> powder in ODS steel volume we consider as fulfilled the following conditions:

1. Nano-particles are not dissolved in stainless steel and create suspension, which means forming of the surface film of iron oxide on their surface.
2. Boundary conditions on the bottom of the convective cell are free as liquid steel with addition of more than 1.5 mass % of ZrO<sub>2</sub> powder create a new phase in relation to pure melt of the metal concentrated in the surface film on the cell bottom.

Horizontal and vertical velocities of mass-transfer in the ECC with non-plane bottom profile and in the absence of nano-particles of ZrO<sub>2</sub> can be determined on Stokes functions (6):

$$v_{r,1,2}(r,z) = -\frac{1}{r} \frac{\partial \psi_{1,2}(r,z)}{\partial z},$$

$$v_{z,1,2}(r,z) = \frac{1}{r} \frac{\partial \psi_{1,2}(r,z)}{\partial r}.$$

The same as in the case, studied in [6], adding of micro and nano- particle of ZrO<sub>2</sub> into the liquid metal subject to convective mass-transfer, will result in impact on this particle of the multi-directional forces: Archimedes lifting force (always directed upwards); gravity force (always directed down); friction force (Stokes force) (directed along the liquid velocity vector).

### 12. Scenario of vacuum-arc melting and convective mixing of ZrO<sub>2</sub> nano-particles

In the vacuum-arc furnace, the material of the cathode in the form of drops, containing nano-particles of ZrO<sub>2</sub> is get-

ting into the central area of the cylindrical convective cell. Here nano-particles are taken upwards by the Archimedes forces and Stokes forces, overcoming the gravity force. Close to the upper boundary of the cell, due to the radial flux, nano-particles are flowing to the crystallizer walls, where by means of Stokes forces and gravity forces are directed to the bottom of the cell. If these forces overcome the Archimedes force, nano-particles get into the closed convective flux and will be subject to convective mixing inside of ECC, which is equal to their even distribution over the volume of the ODS steel sample.

As it is known, the Archimedes force depends on the volume of the particle. Thus the less the volume of the particle  $r_p$  the lower is the buoyancy force. The criterion of overcoming the Archimedes force allows determining micro- and nano-sizes of the particles, at which their even distribution in the cell volume is possible. This criterion is the following [8]:

$$r_p \leq 10^{-2} \sqrt{\frac{9\nu \Delta l}{2g R_c} \frac{\rho_1}{\rho_1 - \rho_p}} \quad (\text{m}), \quad (7)$$

where  $v_c \approx 1 \dots 3$  cm/s is the experimentally measured maximal velocity of liquid metal motion on the upper horizontal surface of the cell;  $\nu$  is the cinematic viscosity of liquid metal;  $g$  is the acceleration of gravity;  $\Delta l$  is the average distance between micro- and nano-particles;  $R_c$  is the radius of the cylindrical convective cell;  $\rho_1$ ,  $\rho_p$  is the density of liquid metal and zirconium dioxide correspondingly.

Despite [8], the criterion (6) is determined by conditional inequality as a sign of equality in (6) is achieved at limiting process to atomic sizes for  $r_p$  and  $\Delta l$ .

As it goes from the equation (7), conventionally spherical particles with radius  $r_p$  (particles have a monoclinic structure [12] in reality), corresponding to inequality will be evenly distributed on the volume of the convective cell.

If the inequality is not realized, the particles will be floating to the surface close to the cell axis and will be taken to the crystallizer surface by the horizontal flux on the upper interface of the cell and thus will be concentrating on the external border of the ODS steel sample.

In conditions of the experiment all nano- or micro-particles of ZrO<sub>2</sub> together with liquid material of the cathode in the form of drops will be moving (injected) in the cell volume, by conditionally marked grey drop-like figures in the upper angle of the cell (Fig. 6). Then, the particles which got into the liquid metal cell will be moving along the current lines inside of the cell (lines II) or the crystallizer wall a (lines I).

Estimation of inequality (7) for experimental conditions shows that ZrO<sub>2</sub> particles with sizes  $r = 80 \dots 100$  nm will be evenly distributed over the ODS steel ingot volume, while for the particles with sizes about 150 nm, their intense ejection on its side surface should be observed.

Based on the described above, the following conclusions can be made:

- the deeper the cathode material gets into the cell (the less the ordinate of the lower boundaries of drop producing figures in Fig. 6), the more evenly ZrO<sub>2</sub> particles are distributed in the cell volume;
- even distribution in the sample volume should be observed for ZrO<sub>2</sub> particles with sizes less than 80–100 nm.

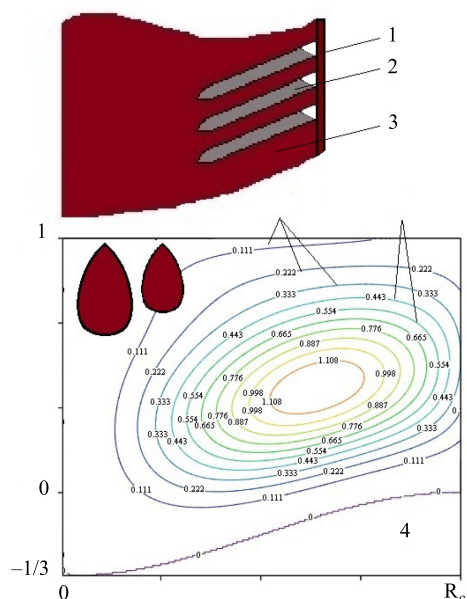


Fig. 6. Scheme of  $ZrO_2$  particles motion in the convective cell. Lines with digitization correspond to current lines: 1 – thin – wall tube, 2 –  $ZrO_2$  powder, 3 – cathode, 4 – cell; I, II – current lines on which the particles are moving

### 13. Conclusions

1. Construction of the cathode of vacuum-arc furnace was offered for the uniform admission of nano – dispersed  $ZrO_2$  powder into the volume of melted metal.

The cathode has a structure of “fish-bone” type in the axial section. Corresponding selection of cathode parameters, taking into account the physical properties of nano-dispersed powder  $ZrO_2$ , provides the uniform admission of the powder into the volume of melted metal.

2. The spatial distribution of convective mass-transfer of the liquid metal in the cylindrical cell with cosine deep bottom profile was described. Calculations show that for model functions, the Stokes lines constitute concentrically placed smoothed, closed lines, whose form reflects curved by the

cosine bottom profile. Such view of the Stokes lines indicates the formation of the convective flux in the form of one vortex in the cell with free boundary conditions.

3. Nano-dispersion  $ZrO_2$  powder particle sizes were determined, at which their spatial homogenization is observed.

Drops of material of the cathode, containing nano-particles of  $ZrO_2$  are getting into the central area of the ECC. Here nano-particles are taken upwards by Archimedes forces and Stokes forces, overcoming the gravity force. Close to the upper boundary of the cell, due to radial flux, nano-particles are flowing to crystallizer walls, where by means of Stokes forces and gravity forces are directed to the bottom of the cell. If these forces overcome the Archimedes force, nano-particles get into the closed convective flux and will be subject to convective mixing inside of ECC, which is equal to their even distribution over the volume of ODS steel sample.

For experimental conditions, it was shown that  $ZrO_2$  nano-particles with sizes, less then 80...100 nm will be evenly distributed over the ODS steel ingot volume.

4. Scenario of vacuum-arc melting and convective homogenization of  $ZrO_2$  nano-particles at production of ODS steel were described.

Drops of material of the cathode with nano-particles of  $ZrO_2$  are entering into the central vertical flow of the ECC. Here particles are exposed to convective mass-transfer, which will result in the impact of the multi-directional forces: Archimedes lifting force (always directed upwards); gravity force (always directed down); friction force (Stokes force) (directed along the liquid velocity vector) on these particles.

The Archimedes force depends on the volume, i. e. size, of the particle. Thus the less the size of the nano-particle the lower is the buoyancy force. Criterion of overcoming the Archimedes force allows determining sizes of the particles, at which their homogeneous distribution in the cell volume is possible.

It is necessary to provide such conditions:

- the deeper the drops get into the cell, the more evenly  $ZrO_2$  particles are distributed in the cell volume;
- even distribution in the sample volume should be observed for  $ZrO_2$  particles with sizes less than 80–100 nm.

### References

1. Libenson, G. A. *Osnovy poroshkovoi metalurgii* [Text] / G. A. Libenson. –M.: «Metallurgy», 1975. – 200 p.
2. Shvedkov, E. L. *Slovar-spravochnik po poroshkovoi metalurgii* [Text] / E. L. Shvedkov, A. T. Denisenko, I. I. Kovenskiy. – Kyiv: Naukova dumka, 1982. – 207 p.
3. *Poroshkovaya metalurgiya v SSSR. Istoriya. Sovremennoe sostoyanie. Perspektivi* [Text] / I. N. Francevich, V. I. Trefilova (Eds.). – Moscow: Nauka, 1986. –166 p.
4. Miller, M. K. High temperature microstructural stability of a MA/ODS ferritic alloy. High temperature alloys: processing for properties, TMS [Electronic resource] / M. K. Miller, D.T. Hoelzer, S.S. Babu, E.A. Kenik, and K. F. Russell. – Oak Ridge, 2003. – Available at: <http://web.ornl.gov/~webworks/cppr/y2001/pres/115155.pdf>
5. Miller, M. K. Nanometer scale precipitation in ferritic MA/ODS alloy MA957 [Text] / M. K. Miller, D. T. Hoelzer, E. A. Kenik, K. F. Russell // J. of Nuclear Materials. – 2004. – Vol. 329-333. – P. 338–341. doi: 10.1016/j.jnucmat.2004.04.085
6. Rogozhkin, S. V. Atom probe characterization of nano-scaled features in irradiated ODS Eurofer steel [Text] / S. V. Rogozhkin, A. A. Aleev, A. G. Zaluzhnyi, A. A. Nikitin, N. A. Iskandarov, P. Vladimirov, R. Lindau, A. Moeslang // Journal of Nuclear Materials. – 2011. – Vol. 409, Issue 2. – P. 94–99. doi: 10.1016/j.jnucmat.2010.09.021

7. Rogozhkin, S. V. Atom probe study of radiation induced precipitates in Eurofer97 Ferritic-Martensitic steel irradiated in BOR-60 reactor [Text] / S. V. Rogozhkin, A. A. Nikitin, A. A. Aleev, A. B. Germanov, A. G. Zaluzhnyi // Inorganic Materials: Applied Research. – 2013. – Vol. 4, Issue 2. – P. 112–118. doi: 10.1134/s2075113313020160
8. Borts, B. V. Research of possibilities of oxide dispersion strengthened (ODS) steels by method of vacuum–arc melting [Text] / B. V. Borts, A. F. Vanzha, I. M. Korotkova, V. I. Sytin, V. I. Tkachenko // PAST. Series «Physics of radiation damages and phenomena in solids». – 2014. – Vol. 4, Issue 92. – P. 117–124.
9. Bozbiei, L. S. Elementary convective cell in the layer of incompressible, viscous liquid and its physical properties [Text] / L. S. Bozbiei, A. O. Kostikov, V. I. Tkachenko // In Proc. of the International conference MSS–14 «Mode conversion, coherent structures and turbulence». – Moscow, 2014.
10. Denisova, E. I. Technology of obtaining zirconium dioxide powders (IV) modified by yttrium (III) and titanium (IV) oxides for plasma heat–proofing coatings [Text]: abstract ... PhD / E. I. Denisova. – Ekaterinburg, Russia, 1998.
11. Chemical reference book. Volume 1. Common information, structure of the substance, properties of the most important substances, laboratory technique [Text] / B. P. Nikolskiy (Ed.). – Moscow–Leningrad, 1966.
12. Kytovoy, V. A. Thermal–vacuum method of obtaining the nano–dispersion materials [Text] / V. A. Kytovoy, Y. G. Kazarinov, A. S. Luzenko, A. A. Nikolaenko, V. I. Tkachenko // PAST. Series «Physics of radiation damages and phenomena in solids». – 2014. – Vol. 2. – P. 153–157.
13. Patochkina, O. L. Elementary Convection Cell in the Horizontal Layer of Viscous Incompressible Liquid with Rigid and Mixed Boundary Conditions [Text] / O. L. Patochkina, B. V. Borts, V. I. Tkachenko // Eastern-European Journal of Physics. – 2015. – Vol. 1. – P. 23–31.
14. Bozbiei, L. S. Heat and mass transfer in the heated from below free cylindrical elementary convection cell with a conical cavity bottom [Text] / L. S. Bozbiei, V. I. Tkachenko // In Proc. of the Intern. Young Sci. Forum on Appl. Phys. YSF–2015. – Dnipropetrovsk, 2015.
15. Tables of physical values [Text] / I. K. Kikoin (Ed.). – Moscow: Atomizdat, 1976. – 1008 p.
16. Sheludyak, Yu. E. Thermal–physical properties of gas systems [Text] / Yu. E. Sheludyak, L. Ya. Kashporov, L. A. Malinin, V. N. Calkov. – Moscow: «Moscow», 1992. – 184 p.
17. Nagaev, E. L. Melkie metalichskie chastici [Text] / E. L. Nagaev // Uspehi fizicheskikh nauk. – 1992. – Vol. 9. – P. 49–124.